

# Photons from jet - plasma interaction in relativistic heavy ion collisions

Lusaka Bhattacharya\* and Pradip Roy†  
Saha Institute of Nuclear Physics, Kolkata - 700064, India

We expose the role of collisional energy loss on high  $p_T$  photon data measured by PHENIX collaboration by calculating photon yield in jet plasma interaction. The phase space distribution of the participating jet is dynamically evolved by solving Fokker-Planck equation. It is shown that the data is reasonably well reproduced when contributions from all the relevant sources are taken into account. Predictions at higher beam energies relevant for LHC experiment have been made.

PACS numbers: 25.75.-q, 12.38.Mh  
Keywords: energy-loss, quark-gluon-plasma

## I. INTRODUCTION

Heavy ion collisions have received significant attention in recent years. Various possible probes have been studied in order to detect the signature of QGP. Study of direct photon and dilepton spectra emanating from hot and dense matter formed in ultra-relativistic heavy ion collisions is a field of considerable current interest. Electromagnetic probes have been proposed to be one of the most promising tools to characterize the initial state of the collisions [1]. Because of the very nature of their interactions with the constituents of the system they tend to leave the system almost unscattered. In fact, photons (dilepton as well) can be used to determine the initial temperature, or equivalently the equilibration time. These are related to the final multiplicity of the produced hadrons in relativistic heavy ion collisions (HIC). By comparing the initial temperature with the transition temperature from lattice QCD, one can infer whether Quark Gluon Plasma (QGP) is formed or not.

There are various sources of photons from relativistic heavy ion collisions: (i) Direct photons are those which are produced in reactions of the type  $ab \rightarrow c\gamma$ . One can subdivide this broad category of "direct photons" into "prompt", "pre-equilibrium", "thermal" (from QGP as well as hadronic phase) and finally the "jet-photon" also called "jet conversion photon" (photons from jet-plasma interaction) depending on their origin. (ii) Decay photons are basically the decay product of long lived secondaries ( $\pi^0 \rightarrow \gamma\gamma$ ,  $\eta \rightarrow \gamma\gamma$ ,  $\rho^0 \rightarrow \pi\pi\gamma$ ,  $\omega \rightarrow \pi\gamma$  etc). The first calculation of thermal photons from quark matter (QM) has been done in Ref. [2] using hard thermal loop (HTL). It is shown that at a fixed temperature the contribution from QM is similar to that produced from hot hadronic matter. Here, our main concern is to calculate the jet-photons and compare them with the thermal photons from QM that has been calculated in Ref. [2].

The jet conversion mechanism [3] occurs when a high energy jet interacts with the medium constituents via

annihilation and Compton processes. It might be noted that this phenomenon (for Compton process) has been illustrated quite some time ago [4] in the context of estimating photons from equilibrating plasma, where, it is assumed that because of the larger cross-section, gluons equilibrate faster providing a heat bath to the incoming quark-jet. A comparison of the photons, calculated in the above scenario, (equivalent to photons from jet-plasma interaction) with the direct photons (thermal) shows that the former remains dominant for photons with  $p_T$  upto 6 GeV [3, 4]. It is to be noted that while evaluating jet-photon it is assumed in Ref. [3] that the largest contribution to photons corresponds to  $p_\gamma \sim p_q(p_{\bar{q}})$ . This implies that the annihilating quark (anti-quark) directly converts into a photon. Moreover, the quark jet might lose energy due to scattering with the constituents of the thermal bath before participating in Compton and annihilation processes. We include this effect on the photon productions.

Collisional energy loss of heavy fermion has been calculated long ago in Ref. [5, 6] using HTL approach. The same for the light quarks and gluons has been discussed in Ref. [7] and revisited recently in Ref. [8]. However, its importance was demonstrated in the context of RHIC in Ref. [9]. The measurements of non-photonic single electron data [10] show larger suppression than expected. These electrons mainly come from heavy quark decay where the radiative energy loss is suppressed due to dead cone effect. This observation has led to re-thinking the importance of collisional energy loss both for heavy as well as light quark [11]. In view of this fact, collisional energy loss has been re-investigated in great detail [11–14] in recent times.

It is argued in Ref. [3] that measurement of photons from such a novel process can provide direct information about the quark momentum. This is because of the assumption made in Ref. [3] that photons are predominantly emitted at  $p_\gamma \sim p_q$ . This implies that the thermal distribution of the participating parton is evaluated at the photon momentum. In this work we relax this assumption and calculate the photon yield from jet-plasma interaction. We consider photon production in the  $p_T$  range  $4 \leq p_T \leq 14\text{GeV}$ . It is to be noted that to produce such photons the required energy of the participating jet

\*Electronic address: lusaka.bhattacharya@saha.ac.in

†Electronic address: pradipk.roy@saha.ac.in

does not exceed (or remains below) the critical energy  $E_c$  ( $E_{\text{rad}} = E_{\text{coll}}$  at  $E = E_c$ ) [8]. In fact, in this energy regime collisional loss seems to play important role [15–17]. It is shown in Ref [15, 17] that the quenching factor for high  $p_T$  hadrons can be accommodated within the framework of collisional energy loss only.

Given the present scenario of energy loss mechanism in the context of RHIC data we, in this work, investigate the role of collisional energy loss as calculated in Refs. [7, 8]. However, in order to see the effects of energy loss on jet-photon one should also incorporate the radiative energy loss and this has to be done in the same formalism in a realistic scenario. This has recently been done in Ref. [18], where it has been shown that the neutral pion  $p_T$  spectra is sensitive to the inclusion of collisional and radiative energy loss.

In the photon production rate (from jet-plasma interaction) one of the collision partners is assumed to be in equilibrium and the other (the jet) is executing random motion in the heat bath provided by quarks (anti-quarks) and gluons. Furthermore, the interaction of the jet is dominated by small angle scattering. In such scenario the evolution of the jet phase space distribution is governed by Fokker-Planck (FP) equation where the collision integral is approximated by appropriately defined drag and diffusion coefficients.

The plan of the paper is as follows. We give a brief description of photon production from QGP in section IIA. The evolution of jet quark and photon  $p_T$  distributions are discussed in sections IIB and IIC respectively. We then briefly mention the necessary formulae for photon production in initial hard collisions in section IID. Section III is devoted to the discussions of results and finally, we summarise in section IV.

## II. FORMALISM

### A. Thermal Photon Rate

The lowest order processes for photon emission from QGP are the Compton scattering ( $q(\bar{q})g \rightarrow q(\bar{q})\gamma$ ) and annihilation ( $q\bar{q} \rightarrow g\gamma$ ) process. The total cross-section diverges in the limit  $t$  or  $u \rightarrow 0$ . These singularities have to be shielded by thermal effects in order to obtain infrared safe calculations. It has been argued in Ref. [19] that the intermediate quark acquires a thermal mass in the medium, whereas the hard thermal loop (HTL) approach of Ref. [20] shows that very soft modes are suppressed in a medium providing a natural cut-off  $k_c \sim gT$ .

We assume that the singularities can be shielded by the introduction of thermal masses for the participating partons. The differential cross-sections for Compton and annihilation processes are given by [21],

$$\frac{d\sigma(qg \rightarrow q\gamma)}{d\hat{t}} = \frac{1}{6} \left(\frac{e_q}{e}\right)^2 \frac{8\pi\alpha_s\alpha_e}{(\hat{s}-m^2)^2} \left[ \left(\frac{m^2}{\hat{s}-m^2} + \frac{m^2}{\hat{u}-m^2}\right)^2 \right.$$

$$\left. + \left(\frac{m^2}{\hat{s}-m^2} + \frac{m^2}{\hat{u}-m^2}\right) - \frac{1}{4} \left(\frac{\hat{s}-m^2}{\hat{u}-m^2} + \frac{\hat{u}-m^2}{\hat{s}-m^2}\right) \right] \quad (1)$$

and

$$\frac{d\sigma(q\bar{q} \rightarrow g\gamma)}{d\hat{t}} = -\frac{4}{9} \frac{8\pi\alpha_s\alpha_e}{\hat{s}(\hat{s}-4m^2)} \left[ \left(\frac{m^2}{\hat{t}-m^2} + \frac{m^2}{\hat{u}-m^2}\right)^2 \right.$$

$$\left. + \left(\frac{m^2}{\hat{t}-m^2} + \frac{m^2}{\hat{u}-m^2}\right) - \frac{1}{4} \left(\frac{\hat{t}-m^2}{\hat{u}-m^2} + \frac{\hat{u}-m^2}{\hat{t}-m^2}\right) \right] \quad (2)$$

where  $m$  is the in-medium thermal quark mass.  $m^2 = 2m_{th}^2 = 4\pi\alpha_s T^2/3$ ,  $\alpha_e$  and  $\alpha_s$  are the electromagnetic fine-structure constant and the strong interaction coupling constant, respectively. The static photon rate in  $1+2 \rightarrow 3+\gamma$  can be written as [1, 2]

$$\frac{dN^\gamma}{d^4x d^2p_T dy} = \frac{\mathcal{N}_i}{(2\pi)^7 E_\gamma} \int d\hat{s} d\hat{t} |\mathcal{M}_i|^2 \times \int dE_1 dE_2 \frac{f_1(E_1) f_2(E_2) (1 \pm f_3(E_3))}{\sqrt{aE_2^2 + 2bE_2 + c}} \quad (3)$$

where

$$a = -(\hat{s} + \hat{t} - m_2^2 - m_3^2)^2$$

$$b = E_1(\hat{s} + \hat{t} - m_2^2 - m_3^2)(m_2^2 - \hat{t})$$

$$+ E[(\hat{s} + \hat{t} - m_2^2 - m_3^2)$$

$$\times (\hat{s} - m_1^2 - m_2^2) - 2m_1^2(m_2^2 - \hat{t})]$$

$$c = E_1^2(m_2^2 - \hat{t})^2 - 2E_1 E[2m_2^2(\hat{s} + \hat{t} - m_2^2 - m_3^2)$$

$$- (m_2^2 - \hat{t})(\hat{s} - m_1^2 - m_2^2)]$$

$$- E^2[(\hat{s} - m_1^2 - m_2^2)^2 - 4m_1^2 m_2^2]$$

$$- (\hat{s} + \hat{t} - m_2^2 - m_3^2)(m_2^2 - \hat{t})$$

$$\times (\hat{s} - m_1^2 - m_2^2) + m_2^2(\hat{s} + \hat{t} - m_2^2 - m_3^2)^2$$

$$+ m_1^2(m_1^2 - \hat{t})^2$$

$$E_{1,min} = \frac{\hat{s} + \hat{t} - m_2^2 - m_3^2}{4E}$$

$$+ \frac{Em_1^2}{\hat{s} + \hat{t} - m_2^2 - m_3^2}$$

$$E_{2,min} = \frac{Em_2^2}{m_2^2 - \hat{t}} + \frac{m_2^2 - \hat{t}}{4E}$$

$$E_{2,max} = -\frac{b}{a} + \frac{\sqrt{b^2 - ac}}{a}$$

$f_1(E_1)$ ,  $f_2(E_2)$  and  $f_3(E_3)$  are the distribution functions of 1st, 2nd and 3rd parton respectively.  $\hat{s}$ ,  $\hat{u}$  and  $\hat{t}$  are the usual Mandelstam variables.  $\mathcal{M}_i$  represents the amplitude for Compton or annihilation process.  $\mathcal{N}_i$  is the overall degeneracy factor. For Compton scattering  $\mathcal{N}_i = 320/3$  and for annihilation process  $\mathcal{N}_i = 20$  when summing over u and d quarks.

### B. Fokker - Planck Equation: Parton transverse momentum spectra

As mentioned already in the introduction that the quark jet here is not in equilibrium. Therefore the corresponding distribution function that appears in Eq. (3)

is calculated by solving the FP equation. The FP equation, can be derived from Boltzmann kinetic equation (BKE) if one of the partner of the binary collisions is in thermal equilibrium and the collisions are dominated by the small angle scattering involving soft momentum exchange [9, 22–27].

To arrive at the relevant FP equation from BKE we assume that there is no external force and therefore,

$$\left(\frac{\partial}{\partial t} + \mathbf{v}_{\mathbf{p}} \cdot \nabla_{\mathbf{r}}\right) f(\mathbf{p}, \mathbf{x}, t) = C[f(\mathbf{p}, \mathbf{x}, t)] \quad (4)$$

Here, quarks have a phase space distribution which evolves in time and the collision term is evaluated by considering ultra-relativistic scattering of the quarks and gluons which eventually are expressed in terms of transport coefficients. For a Bjorken expansion [28] the probability distribution is independent of the transverse coordinates and invariant under boosts in the  $z$ -direction and Eq. (4) is considerably simplified. Considering that the system expands in the longitudinal direction Eq. (4) takes the following form [29]:

$$\frac{\partial f(\mathbf{p}, z, t)}{\partial t} + v_{pz} \frac{\partial f(\mathbf{p}, z, t)}{\partial z} = C[f(\mathbf{p}, z, t)]. \quad (5)$$

Here,  $v_{pz} = p_z/E_p$  (for light partons  $E_p = |p|$ ). This equation can be simplified further for the central rapidity region which is boost invariant in rapidity, which implies

$$f(\mathbf{p}_{\mathbf{T}}, p_z, z, t) = f(\mathbf{p}_{\mathbf{T}}, p'_z, \tau). \quad (6)$$

Here  $p'_z = \gamma(p_z - u_z p)$ , the transformation velocity  $u_z = z/t$ ,  $\gamma = (1 - u_z^2)^{-1/2} = t/\tau$  and  $\tau = \sqrt{t^2 - z^2}$  denotes the proper time. Using the Lorentz transformation relation  $\partial\tau/\partial z|_{z=0} = 0$ ,  $\gamma_{z=0} = 1$  and  $\partial p'_z/\partial z|_{z=0} = -p/t$ , one finds

$$v_{pz} \frac{\partial f}{\partial z} = -\frac{p_z}{t} \frac{\partial f}{\partial p_z} \quad (7)$$

Therefore the Boltzmann equation takes the following form

$$\frac{\partial f(\mathbf{p}_{\mathbf{T}}, p_z, t)}{\partial t} \Big|_{p_z t} = \left(\frac{\partial}{\partial t} - \frac{p_z}{t} \frac{\partial}{\partial p_z}\right) f(\mathbf{p}_{\mathbf{T}}, p_z, t) \quad (8)$$

$$\left(\frac{\partial}{\partial t} - \frac{p_z}{t} \frac{\partial}{\partial p_z}\right) f(\mathbf{p}_{\mathbf{T}}, p_z, t) = C[f(\mathbf{p}_{\mathbf{T}}, p_z, t)]. \quad (9)$$

Evidently in Eq. (9), the second term on the left hand side represents the expansion while the right hand side characterizes the collisions. The latter can be written in terms of the differential collision rate  $W_{\mathbf{p}, \mathbf{q}}$

$$C[f(\mathbf{p}_{\mathbf{T}}, p_z, t)] = \int d^3 q [W_{p+q; q} f(\mathbf{p} + \mathbf{q}) - W_{p; q} f(\mathbf{p})] \quad (10)$$

which quantifies the rate of change of the quark momentum from  $\mathbf{p}$  to  $\mathbf{p} - \mathbf{q}$ ,  $W_{\mathbf{p}, \mathbf{q}} = d\Gamma(\mathbf{p}, \mathbf{q})/d^3 q$ , where  $\Gamma$  represents scattering rates.

In a partonic plasma, small angle collisions, with parametric dependence of  $O(g^2 T)$ , are more frequent than the large angle scattering rate. The latter goes as  $\sim O(g^4 T)$ . Therefore the distribution function does not change much over the mean time between two soft scatterings. This allows us to approximate  $f(\mathbf{p} + \mathbf{q}) \simeq f(\mathbf{p})$ . In contrast,  $W_{\mathbf{p}, \mathbf{q}}$ , being sensitive to small momentum transfer, falls off very fast with increasing  $q$ . Therefore, we write

$$W_{\mathbf{p}+\mathbf{q}, \mathbf{q}} f(\mathbf{p} + \mathbf{q}) \simeq W_{\mathbf{p}, \mathbf{q}} f(\mathbf{p}) + q_i \frac{\partial}{\partial p_i} (W_{\mathbf{p}, \mathbf{q}} f) + \frac{1}{2} q_i q_j \frac{\partial^2}{\partial p_i \partial p_j} (W_{\mathbf{p}, \mathbf{q}} f) \quad (11)$$

With these approximation, Eq. 9 can be written as

$$\left(\frac{\partial}{\partial t} - \frac{p_z}{t} \frac{\partial}{\partial p_z}\right) f(\mathbf{p}_{\mathbf{T}}, p_z, t) = \frac{\partial}{\partial p_i} A_i(\mathbf{p}) f(\mathbf{p}) + \frac{1}{2} \frac{\partial}{\partial p_i \partial p_j} [B_{ij}(\mathbf{p}) f(\mathbf{p})], \quad (12)$$

where we have defined the following kernels,

$$A_i = \int d^3 q W_{\mathbf{p}, \mathbf{q}} q_i \quad (13)$$

$$B_{ij} = \int d^3 q W_{\mathbf{p}, \mathbf{q}} q_i q_j \quad (14)$$

Writing  $A_i = p_i \eta$  and  $B_{ij} = B_t (\delta_{ij} - \frac{p_i p_j}{p^2}) + B_l \frac{p_i p_j}{p^2}$  we arrive at the following equation

$$\left(\frac{\partial}{\partial t} - \frac{p_z}{t} \frac{\partial}{\partial p_z}\right) f(\mathbf{p}, t) = \frac{\partial}{\partial p_i} [p_i \eta f(\mathbf{p}, t)] + \frac{1}{2} \frac{\partial^2}{\partial p_z^2} [B_l(\mathbf{p}) f(\mathbf{p}, t)] + \frac{1}{2} \frac{\partial^2}{\partial p_T^2} [B_t f(\mathbf{p}, t)] \quad (15)$$

In Eq. (15)  $f(\mathbf{p}, t)$  represents the non-equilibrium distribution of the partons under study,  $\eta = (1/E) dE/dx$ , denotes drag coefficient,  $B_l = d\langle(\Delta p_z)^2\rangle/dt$ ,  $B_t = d\langle(\Delta p_T)^2\rangle/dt$ , represent diffusion constants along parallel and perpendicular directions of the propagating partons.

The transport coefficients,  $\eta$ ,  $B_l$  and  $B_t$  appeared in Eq. (15) can be calculated from the following expressions:

$$\frac{dE}{dx} = \frac{\nu_i}{(2\pi)^5} \int \frac{d^3 k d^3 q d\omega}{2k 2k' 2p 2p'} \delta(\omega - \mathbf{v}_{\mathbf{p}} \cdot \mathbf{q}) \delta(\omega - \mathbf{v}_{\mathbf{k}} \cdot \mathbf{q}) \times \langle \mathcal{M} \rangle_{i \rightarrow 0}^2 f(|\mathbf{k}|) [1 \pm f(|\mathbf{k} + \mathbf{q}|)] \omega \quad (16)$$

$$B_{t, l} = \frac{\nu_i}{(2\pi)^5} \int \frac{d^3 k d^3 q d\omega}{2k 2k' 2p 2p'} \delta(\omega - \mathbf{v}_{\mathbf{p}} \cdot \mathbf{q}) \delta(\omega - \mathbf{v}_{\mathbf{k}} \cdot \mathbf{q}) \times \langle \mathcal{M} \rangle_{i \rightarrow 0}^2 f(|\mathbf{k}|) [1 \pm f(|\mathbf{k} + \mathbf{q}|)] q_{t, l}^2 \quad (17)$$

in the small angle limit [8, 9]. Here  $f(|\mathbf{k}|, t)$  denotes the thermal distributions for the quarks (Fermi-Dirac) or gluons (Bose-Einstein) and  $\nu_i$  stands for the statistical degeneracy factor for the  $i^{\text{th}}$  parton species. The matrix

elements required to calculate the transport coefficients include diagrams involving exchange of massless gluons which render  $dE/dx$  and  $B_{l,t}$  infrared divergent. Such divergences can naturally be cured by using HTL [20] corrected propagator for the gluons, i.e. the divergence is shielded by plasma effects.

In the coulomb gauge the gluon propagator for the transverse and longitudinal modes are denoted by  $D_{00} = \Delta_l$  and  $D_{ij} = (\delta_{ij} - q^i q^j / q^2) \Delta_t$  with [30]:

$$\Delta_l(q_0, q)^{-1} = q^2 - \frac{3}{2} \omega_p^2 \left[ \frac{q_0}{q} \ln \frac{q_0 + q}{q_0 - q} - 2 \right] \quad (18)$$

$$\begin{aligned} \Delta_t(q_0, q)^{-1} &= q_0^2 - q^2 + \frac{3}{2} \omega_p^2 \\ &\times \left[ \frac{q_0(q_0^2 - q^2)}{2q^3} \ln \frac{q_0 + q}{q_0 - q} - \frac{q_0^2}{q^2} \right] \end{aligned} \quad (19)$$

The HTL modified matrix element in the limit of small angle scattering takes the following form [8, 9] for all the partonic processes having dominant small angle contributions like  $qg \rightarrow qg$ ,  $qq \rightarrow qq$  etc.:

$$\begin{aligned} |\mathcal{M}|^2 &= g^4 C_R 16 (E_p E_k)^2 |\Delta_l(q_0, q) \\ &+ (\mathbf{v}_p \times \hat{q}) \cdot (\mathbf{v}_k \times \hat{q}) \Delta_t(q_0, q)|^2 \end{aligned} \quad (20)$$

where  $C_R$  is the appropriate color factor. With the screened interaction, the drag and diffusion constants can be calculated along the line of Ref. [9]. For jet with energy  $E \gg T$  Eqs.(5) and (6), in leading log approximation, give (e.g. for  $qg \rightarrow qg$ ) [8]

$$\begin{aligned} \frac{dE}{dx} &= \frac{\nu_q \pi \alpha_s^2 T^2}{6} \ln \left( \frac{E}{g^2 T} \right) \\ B_t &= \frac{2\nu_q \pi \alpha_s^2 T^3}{3} \ln \left( \frac{E}{g^2 T} \right) \\ B_l &= \frac{\nu_q \pi \alpha_s^2 T^3}{3} \ln \left( \frac{E}{g^2 T} \right) \end{aligned} \quad (21)$$

Similarly, drag and diffusion coefficients for the relevant processes can be calculated analogously. Having known the drag and diffusion, we solve the FP equation using Green's function techniques: If  $P(\vec{p}, t | \vec{p}_0, t_i)$  is a solution to Eq.(15) with the initial condition

$$P(\vec{p}, t = t_i | \vec{p}_0, t_i) = \delta^{(3)}(\vec{p} - \vec{p}_0) \quad (22)$$

the full solution with an arbitrary initial condition can be obtained as [24]

$$f(t, \vec{p}) = \int d^3 \vec{p}_0 P(\vec{p}, t | \vec{p}_0, t_i) f_0(\vec{p}_0) \quad (23)$$

where for the initial condition  $f(t = 0, \vec{p}) = f_0(p_0)$  and  $P(\vec{p}, t | \vec{p}_0, t_i)$  is the Green's function of the partial differential Eq.(15).

Thus, to obtain  $p_T$  distribution of the jets at time  $t$  we need to convolve the Green's function with the initial spectrum [27]:

$$E \frac{dN}{d^3 p} (p_T, t) = \int d^3 p_0 P(\vec{p}, t | \vec{p}_0, t_i) E_0 \frac{dN}{d^3 p_0} \quad (24)$$

We use the initial parton  $p_T$  distributions (at the formation time  $t_i$ ) taken from [3, 31]:

$$\frac{dN}{d^2 p_{0T} dy_0} \Big|_{y_0=0} = \frac{K N_0}{(1 + \frac{p_{0T}}{\beta})^\alpha}, \quad (25)$$

where  $K$  is a phenomenological factor ( $\sim 1.5 - 2$ ) which takes into account the higher order effects. The values of the parameters are listed in Table. I.

	RHIC		LHC	
	$q$	$\bar{q}$	$q$	$\bar{q}$
$N_0$ [ $1/GeV^2$ ]	$5.0 \times 10^2$	$1.3 \times 10^2$	$1.4 \times 10^4$	$1.4 \times 10^5$
$\beta$ [GeV]	1.6	1.9	0.61	0.32
$\alpha$	7.9	8.9	5.3	5.2

TABLE I: Parameters for initial parton  $p_T$  distribution.

### C. Space time evolution

In this section we discuss how to obtain the space-time integrated rate of photons from jet plasma interaction using Bjorken hydrodynamics [28]. Note that, for jet photon, one of the distribution function appearing in Eq.(3) should be replaced by the phase-space distribution of the incoming jet. We assume invariant Bjorken correlation [32] between the particle rapidity ( $y$ ) and the space time rapidity ( $\eta$ ) to obtain the phase phase distribution of the jet. Now we have

$$\nu_i \int \frac{d^3 x d^3 p}{(2\pi)^3} f(x, p) = N_i \quad (26)$$

where  $N_i$  is the number of particles  $i$  and  $\nu_i$  is the spin-color degeneracy. The phase-space distribution function for an incoming (quark) jet, assuming Bjorken  $\eta - y$  correlation [32], is as follows,

$$\begin{aligned} f_{jet}(\vec{r}, \vec{p}, t_i) &= \frac{(2\pi)^3 \mathcal{P}(r_\perp)}{\nu_q \tau p_T} \frac{dN}{d^2 p_T dy} \delta(\eta - y) \\ &= \frac{(2\pi)^3 \mathcal{P}(r_\perp) t_i p_T}{\nu_q \sqrt{t_i^2 - z_0^2} E^2} \frac{dN}{d^2 p_T dy} \delta(z_0 - v_z t_i) \end{aligned} \quad (27)$$

where,  $t_i$  is the formation time of the jet, and  $z_0$  is its position in the QGP expansion direction. We consider the jets to be massless. It is also assumed that the jets do not change direction due to its interaction with the

plasma particles. In such case  $f_{jet}$  can be factorized into a position space and a momentum space part and finally we obtain the phase space distribution of the jet at a later time  $t'$  and at  $y = 0$  as (see Ref. [33] for details),

$$f_{jet}(\vec{r}, \vec{p}, t')|_{y=0} = \frac{(2\pi)^3 \mathcal{P}(|\vec{w}_r|) t_i}{\nu_q \sqrt{t_i^2 - z_0^2}} \frac{1}{p_T} \times \frac{dN}{d^2 p_T dy}(p_T, t') \delta(z_0) \quad (28)$$

where  $\frac{dN}{d^2 p_T dy}(p_T, t')$  can be obtained from Eq.(24).  $\nu_q$  is the spin-color degeneracy factor for the incoming quark and  $\mathcal{P}(|\vec{w}_r|)$  is the initial jet production probability distribution at the initial radial position  $\vec{w}_r$  in the plane  $z_0 = 0$ , where

$$|\vec{w}_r| = (\vec{r} - (t' - t_i) \frac{\vec{p}}{|\vec{p}|}) \cdot \hat{r} = \sqrt{(r \cos \phi - t')^2 + r^2 \sin^2 \phi} \text{ for } t_i \sim 0 \quad (29)$$

and  $\phi$  is the angle in the plane  $z_0 = 0$  between the direction of the photon and the position where this photon has been produced. We assume the plasma expands only longitudinally. Thus using  $d^4 x = r dr dt' d\phi dz_0$  we obtain the transverse momentum distribution (using Eqs.(3) and (28)) of photon as follows:

$$\begin{aligned} \frac{dN^\gamma}{d^2 p_T dy} &= \int d^4 x \frac{dN^\gamma}{d^4 x d^2 p_T dy} \\ &= \frac{(2\pi)^3}{\nu_q} \int_{t_i}^{t_c} dt' \int_0^R r dr \int d\phi \mathcal{P}(\vec{w}_r) \\ &\times \frac{\mathcal{N}_i}{16(2\pi)^7 E_\gamma} \int d\hat{s} d\hat{t} |\mathcal{M}_i|^2 \int dE_1 dE_2 \\ &\times \frac{1}{p_{1T}} \frac{dN}{d^2 p_{1T} dy}(p_{1T}, t') \frac{f_2(E_2)(1 \pm f_3(E_3))}{\sqrt{aE_2^2 + 2bE_2 + c}} \end{aligned} \quad (30)$$

where  $\frac{dN}{d^2 p_{1T} dy}(p_{1T}, t')$  can be calculated from Eq.(24).  $f_2, f_3$  are Fermi-Dirac or Bose-Einstein distributions.  $t_c$  is the time when phase transition from quark matter (QM) to hadronic matter (HM) begins and can be obtained by using Bjorken cooling law [28].  $R$  is the transverse dimension of the system.  $\phi$  dependence occurs only in  $\mathcal{P}(\vec{w}_r)$ . So the  $\phi$  integration can be done analytically as in Ref. [33]. The temperature profile is taken from Ref. [33].

#### D. Hard Photons

The large  $p_T$ -phenomenon in hadron-hadron collisions is well described by the perturbative QCD (pQCD) improved parton model. In this model it is assumed that the partonic structures of hadrons are revealed at high energies. The strong coupling constant  $\alpha_s$  becomes ‘weak’

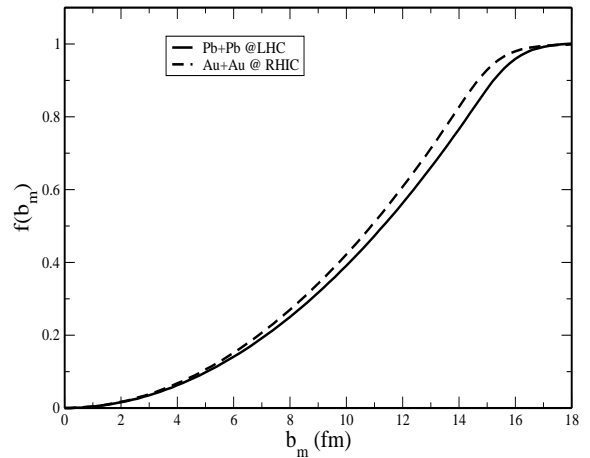


FIG. 1: Centrality fraction as a function of maximum impact parameter  $b_m$ .

so that perturbative expansion in powers of  $\alpha_s$  becomes meaningful. Thus the partonic cross-section, reaction rates etc. can be calculated without much ambiguity and with great degree of accuracy. Therefore, within this model the hard photons coming from initial hard parton-parton collisions can be estimated very accurately.

In order to calculate reaction of the type  $h_A h_B \rightarrow \gamma X$  (where  $h_A, h_B$  refer to hadrons), we assume that the energy is such that the partonic degrees of freedom become relevant and they behave incoherently. The cross-section for this process can then be written in terms of elementary parton-parton cross-section multiplied by the partonic flux which depends on the parton distribution functions [34]. The energy scale (so-called factorization scale) for this to happen is denoted by  $Q^2$ , the square of the momentum transfer of the reaction. Starting with two body scattering at the partonic level the differential cross-section for the reaction of above type can be written as [35]

$$\begin{aligned} \frac{d\sigma_{\gamma, \text{hard}}}{d^2 p_T dy} &= K \sum_{abc} \int_{x_a^{\min}}^1 dx_a G_{a/h_A}(x_a, Q^2) G_{b/h_B}(x_b, Q^2) \\ &\times \frac{2}{\pi} \frac{x_a x_b}{2x_a - x_T e^y} \frac{d\sigma}{dt}(ab \rightarrow \gamma c). \end{aligned} \quad (31)$$

where,  $x_T = 2p_T/\sqrt{s}$ . The elementary partonic cross-sections for Compton scattering and annihilation process are given earlier. We also include photons from frag-

mentation process. This is accomplished by introducing the fragmentation function,  $D_{\gamma/c}(z, Q^2)$ , when multiplied by  $dz$  gives the probability for obtaining a photon from parton  $c$ . Here  $z$  is fractional momentum carried by the photon. The differential cross-section is, therefore [35],

$$\frac{d\sigma_{\gamma, \text{frag}}}{d^2 p_T dy} = K \sum_{abcd} \int_{x_a^{\min}}^1 dx_a \int_{x_b^{\min}}^1 G_{a/h_A}(x_a, Q^2)$$



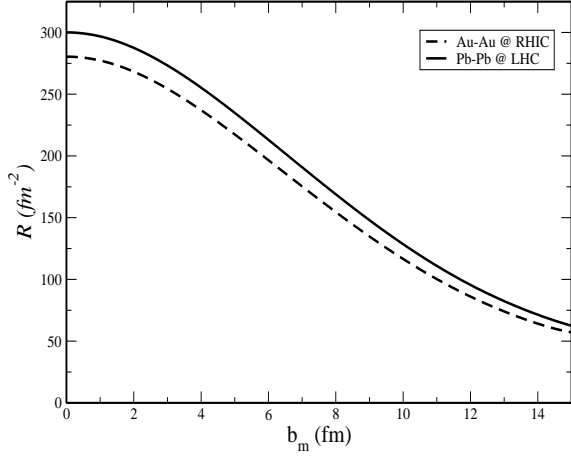


FIG. 2:  $\mathcal{R}$  as a function of maximum impact parameter  $b_m$  corresponding to RHIC and LHC.

$$\begin{aligned} & \times G_{b/h_B}(x_b, Q^2) D_{\gamma/c}(z, Q^2) \\ & \times \frac{1}{\pi z} \frac{d\sigma}{dt}(ab \rightarrow cd), \end{aligned} \quad (32)$$

where

$$\begin{aligned} z &= \frac{x_T}{2x_b} e^y \\ x_b^{\min} &= \frac{x_a x_T e^{-y}}{2x_a - x_T e^y} \\ x_a^{\min} &= \frac{x_T e^y}{2 - x_T e^{-y}} \end{aligned} \quad (33)$$

Once the photon production cross-section is obtained

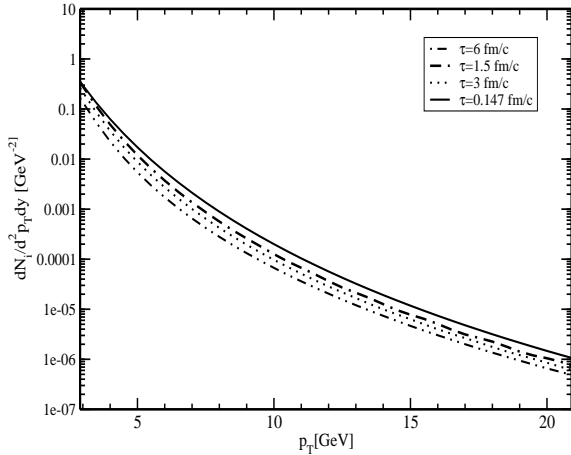


FIG. 3:  $p_T$  distribution of light flavors. The parameters (such as initial temperature  $T_i$  and time  $\tau_i$ ) correspond to RHIC experiment.  $T_i = 0.446$  GeV and  $\tau_i = 0.147$  fm/c.

from hadron-hadron collision we can now determine the direct photon production rates due to hard scattering

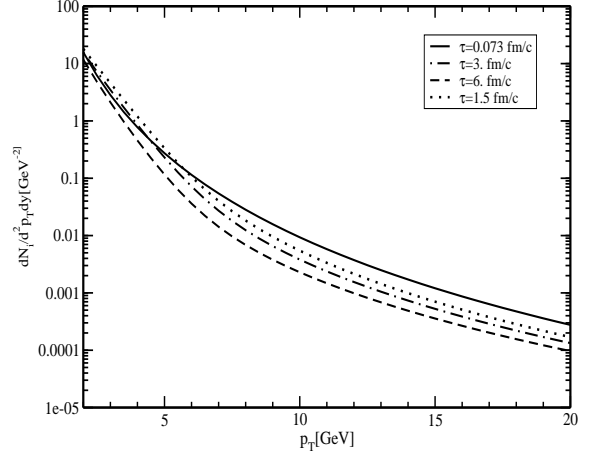


FIG. 4: Same as Fig.(3) at LHC.  $T_i = 0.897$  GeV and  $\tau_i = 0.073$  fm/c.

between partons from nucleus-nucleus collisions at relativistic energies. To do this we must note that the experimental data are given for a particular centrality. In order to take into account this experimental fact we introduce the centrality parameter (or the most inelastic fraction). It depends on the maximum impact parameter  $b_m$  an can be calculated from the expression:

$$f(b_m) = \frac{\int_0^{b_m} d\mathbf{b} (1 - [1 - T_{AB}(b)\sigma_{NN}^{in}]^{AB})}{\int_0^\infty d\mathbf{b} (1 - [1 - T_{AB}(b)\sigma_{NN}^{in}]^{AB})} \quad (34)$$

From this expression we extract  $b_m$  relevant for a given experiment and use it to calculate photons from initial hard collisions and from parton fragmentation. Thus the yield becomes

$$\frac{dN_{AB}}{d^2 p_T dy}(b_m) = \mathcal{R}(b_m) \left[ \frac{d\sigma_{\gamma, \text{hard}}}{d^2 p_T dy} + \frac{d\sigma_{\gamma, \text{frag}}}{d^2 p_T dy} \right] \quad (35)$$

where

$$\mathcal{R}(b_m) \equiv \langle AB T_{AB} \rangle = \frac{\int_0^{b_m} d^2 \mathbf{b} AB T_{AB}(b)}{\int_0^{b_m} d\mathbf{b} (1 - [1 - T_{AB}(b)\sigma_{NN}^{in}]^{AB})} \quad (36)$$

and

$$T_{AB}(\mathbf{b}) = \int d^2 \mathbf{s} T_A(\mathbf{s}) T_B(\mathbf{b} - \mathbf{s}), \quad (37)$$

is the nuclear overlap function.

### III. RESULTS

First of all let us concentrate on the centrality measurements in an experiment. The photon measurement is done for a given centrality. For example, 10% centrality corresponds to  $f(b_m) \sim 0.1$ . In Fig. 1 we plot

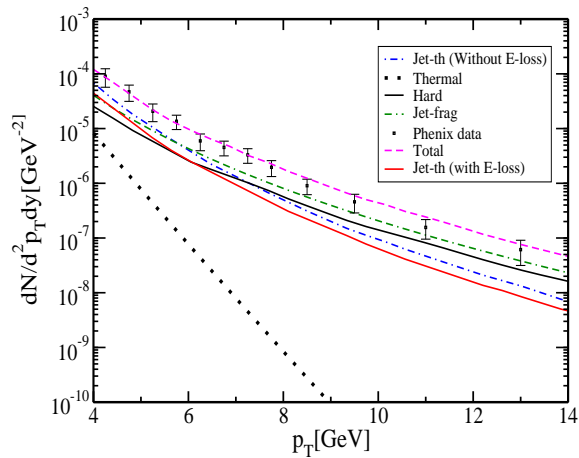


FIG. 5: (Color online)  $p_T$  distribution of photons at RHIC energies. The red (blue) curve denotes the photon yield from jet-plasma interaction with (without) energy loss. The solid (dotted) black curve corresponds to hard (thermal) photons. The magenta represents the total yield compared with the Phenix measurements of photon data [36].  $T_i = 0.446$  GeV and  $t_i = 0.147$  fm/c

the most inelastic fraction as a function of the maximum impact parameter  $b_m$  for Pb-Pb collisions at LHC. We obtain  $b_m \sim 5$  fm for 10% most central collision for Pb-Pb system. Similar value is obtained for RHIC.  $\mathcal{R}$  vs  $b_m$  given by Eq. 36 is plotted in Fig. 2 for Pb-Pb and Au-Au systems from which we obtain  $\mathcal{R} \sim 215(235)$  fm $^{-2}$  at RHIC (LHC) for 10% centrality. We shall use these values while estimating hard photon yields at RHIC (LHC) energies. We plot the transverse momentum distributions of quarks in Figs. 3 and 4 for different times at RHIC and LHC energies respectively where the initial distributions are taken from Eq. (28). It is seen that as the time increases the quark stays longer in the medium losing more energy. As a result the depletion in the distribution function is clearly revealed. It should be noted here that we do not include the induced gluon radiation which may further deplete the distribution at higher momenta.

In Fig. 5 we show the  $p_T$  distribution of photons from various processes which contribute at this high  $p_T$  range. It is observed that due to the inclusion of energy loss in the jet-plasma interaction the yield is depleted. Our calculation without energy loss is similar to that in Ref. [3] at RHIC energies. However, at LHC energies, as we shall see below, the difference is by a factor of 2–3. Thus, we see that the assumption made in Ref [3] could be valid for RHIC energies in the  $p_T$  range considered here, but at higher beam energies this is not a good approximation. It is observed from Fig. 5 due to the inclusion of energy loss the rate is lowered by a factor  $\sim 1.5(1.7)$  at  $p_T = 4(14)$ . This is more or less similar to what is obtained in Ref. [33]. The total photon yield consists of jet-photon, photons from initial hard collisions, jet-fragmentation and thermal photons. It is seen that Phenix photon data is well reproduced in our model. At

high  $p_T$  region the data is marginally reproduced. The reason behind this is the following. For high  $p_T$  photon the incoming jet must have high energy where the radiative loss starts to dominate. Inclusion of this mechanism might lead to a better description of the data in high  $p_T$  range. In order to understand the role of photons from

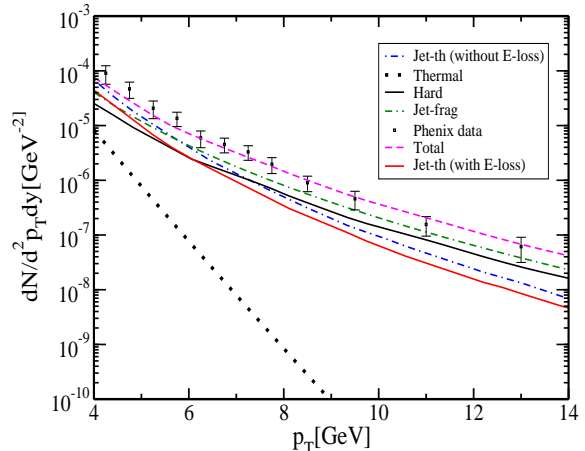


FIG. 6: (Color online) Same as Fig. (5) where in the total yield the contribution of photons from jet plasma interaction has been excluded.

jet-plasma interaction in describing the Phenix high  $p_T$  photon data we show in Fig. 6 where the contribution from jet-plasma interaction is excluded. It is seen that in order to reproduce the data with  $3 < p_T < 6$  GeV one must consider this extra source of photons.

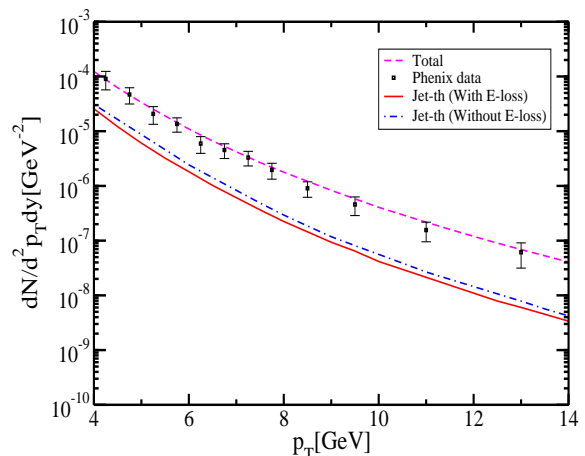


FIG. 7: (Color online)  $p_T$  distribution of photons at RHIC energies with  $T_i = 0.350$  GeV and  $\tau_i = 0.25$  fm/c. The magenta line corresponds to total yield from all the sources as in Fig. (5) with energy loss included in the jet-photon contribution.

To cover the uncertainties in the initial conditions for a given beam energy, we consider another set of initial conditions at a lower temperature  $T_i = 0.350$  GeV and somewhat later initial time of  $\tau_i = 0.25$  fm/c. The yield for this set is shown in Fig. 7. We see that the data is reproduced reasonably well. The inclusion of radiative energy loss will improve the situation further.

As mentioned before, we also consider the high  $p_T$  photon production at LHC energies. The contributions from various sources are shown in Fig. 7. Since the initial temperature in this case is higher, the plasma lives for longer time. Thus the energy loss suffered by the parton is more. As a result, the difference between the cases with and without energy loss is slightly more than what is obtained at RHIC. We do not consider strange quark as it

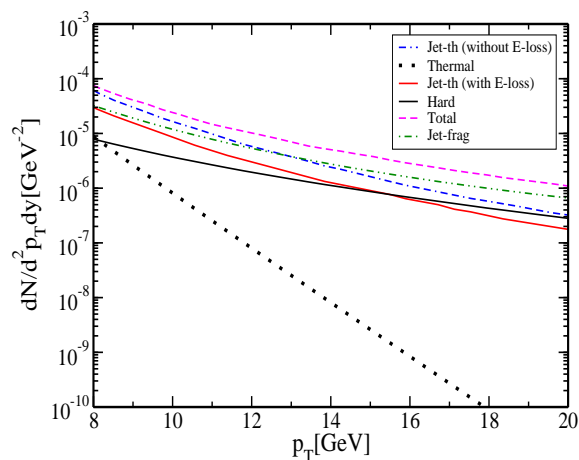


FIG. 8: (Colour online) Same as Fig.(5) at LHC energies.  $T_i = 0.897$  GeV and  $\tau_i = 0.073$  fm/c.

is Boltzmann suppressed because of its high mass. However, if one considers strange quark the effective number of flavours is taken as 2.5. For  $N_F = 2(2.5)$  the lifetime of the plasma ( $t_c - t_i$ ) is of the order of  $1.9(2.6)$  fm/c (the values of  $T_c$  are taken from Ref. [37]). So we see that the life of the plasma increases marginally. As a result minor enhancement in the yield is expected. On the other hand, the degeneracy factor  $\mathcal{N}_i$  is  $20(30)$   $N_F = 2(2.5)$  in case of annihilation processes. So the yield will be larger by a factor of the order of 1.5. Similar thing happens in the case of compton scattering.

#### IV. SUMMARY

We have calculated the transverse momentum distribution of photons from jet plasma interaction with collisional energy loss. It is shown that the assumption made in Ref. [3] while calculating photons from jet - plasma interactions may not be good at LHC energies (the difference is by a factor of 2 – 3). Phenix photon data have been contrasted with the present calculation and the data seem to have been reproduced well. We note that the yield of thermal photons as well as photons from jet-plasma interaction is very sensitive to initial temperature ( $T_i$ ) time ( $\tau_i$ ) and the equation of state. It is shown that in order to describe the Phenix data in the domain  $4 < p_T < 14$  GeV the contribution from jet-plasma interaction is found to be important. The energy of the jet quark to produce photons in this range is such that collisional energy loss plays a dominant role here. In view of this fact we have considered collisional energy loss only. However, one should include both mechanisms in a consistent manner to describe the high  $p_T$  data beyond 14 GeV or so. We note that the data is over-predicted unless the energy loss is included. As we validate our model through the description of Phenix data we also predict the high  $p_T$  photon yield that might be expected in the future experiment at LHC. We observe that the contribution from jet-plasma interaction is slightly more reduced as compared to the RHIC case. We notice that the inclusion of the radiative energy loss will further reduce the yield at high  $p_T$ . That is expected to give a better description of the Phenix data in the high energy regime.

Finally, it should be noted that the fragmentation photon should, in principle, be calculated taking into account the energy loss of the fragmenting parton while traversing the plasma. This can be done by calculating the modified  $p_T$  distribution of the parton by using FP equation and then fragmenting it into photon as is done in case of high  $p_T$  hadron production in relativistic heavy ion collisions [17]. The yield will be depleted as compared to the result shown in the present work. This can lead to the situation where jet-photons and fragmentation photons may be comparable in the intermediate  $p_T$  domain as is evident from the present results. However, in the present work we do not consider this aspect as our main concern is to see the effect of collisional energy loss on photons from jet plasma interaction.

- 
- [1] J. Alam, S. Sarkar, P. Roy, T. Hatsuda and B. Sinha, Ann. Phys. **286**, 159 (2000).
  - [2] J. I. Kapusta, P. Litchard and D. Seibert, Phys. Rev. D **44**, 2774 (1991).
  - [3] R. J. Fries, B. Muller, and D. K. Srivastava, Phys. Rev. Lett. **90**, 132301 (2003).
  - [4] P. Roy, J. Alam, S. Sarkar, B. Sinha, and S. Raha, Nucl. Phys. A **624**, 687 (1997).
  - [5] E. Braaten and M. H. Thoma, Phys. Rev. D **44**, 1298 (1991).
  - [6] E. Braaten and M. H. Thoma, Phys. Rev. D **44**, 2625 (1991).
  - [7] M. H. Thoma, Phys. Lett. **B273**, 128 (1991).
  - [8] A. K. Dutt-Mazumder, J. Alam, P. Roy, B. Sinha, Phys. Rev. D **71**, 094016 (2005).
  - [9] P. Roy, A. K. Dutt-Mazumder and J. Alam, Phys. Rev.



- C **73**, 044911 (2006).
- [10] S. S. Adler et al., Phenix Collaboration, Phys. Rev. Lett. **96**, 032301 (2006).
- [11] A. Adil, M. Gyulassy, W. Horowitz and S. Wicks, Phys. Rev. C **75** 044906 (2007); M. Djordjevic, Phys. Rev. C **74** 064907 (2006); T. Renk, Phys. Rev. C **76** 064905 (2007).
- [12] S. Peigne, P. B. Gossiaux, and T. Gousset, J. High energy Phys. **04**, 011 (2006).
- [13] J. Braun and H-J. Pirner, Phys. Rev. D **75**, 054031 (2007).
- [14] A. Ayala, J. Magnin, L. M. Montano, and E. Rojas, Phys. Rev. C **77**, 044904 (2008).
- [15] M. G. Mustafa and M. H. Thoma, Acta Phys. Hung. A **22**, 93 (2005).
- [16] A. Peshier, Phys. Rev. C **75**, 034906 (2007).
- [17] P. Roy, J. Alam and A. K. Dutt-Mazumder, J. Phys. G **35**, 104047 (2008).
- [18] G. Y. Qin, J. Ruppert, C. Gale, S. Jeon, G. Moore, and M. G. Mustafa, Phys. Rev. Lett **100**, 072301 (2008).
- [19] K. Kajantie and P. V. Ruskanen Phys. Lett. **B121**, 352 (1983).
- [20] R. D. Pisarski and E. Braaten, Nucl. Phys. **B337**, 569 (1990); *ibid* Nucl. Phys. **B339**, 310 (1990).
- [21] C. Y. Wong, Introduction to High Energy Heavy Ion Collisions, 1994, World Scientific, Singapore.
- [22] J. Alam, S. Raha and B. Sinha, Phys. Rev. Lett **73**, 1895 (1994).
- [23] B. Svetitsky, Phys. Rev. D **37**, 2484 (1988).
- [24] G. D. Moore and D. Teaney, Phys. Rev. C **71**, 064904 (2005).
- [25] M. B. G. Ducati, V. P. Goncalves and L. F. Mackedanz, hep-ph/0506241.
- [26] J. BJORAKER and R. Venugopalan, Phys. Rev. C **63**, 024609 (2001).
- [27] H. V. Hees and R. Rapp, Phys. Rev. C **71** 034907 (2005).
- [28] J. D. Bjorken, Phys. Rev. D **27** 140 (1983).
- [29] G. Baym, Phys. Lett. B **138** 18 (1984).
- [30] M. Le Bellac, Thermal Field Theory, Cambridge University Press, Cambridge, 1996.
- [31] B. Muller, Phys. Rev. C **67** 061901R (2003).
- [32] Z. Lin and M. Gyulassy, Phys. Rev. C **51**, 2177 (1995).
- [33] S. Turbide, C. Gale, S. Jeon and G. D. Moore, Phys. Rev. C **72** 014906 (2005).
- [34] J. PUMPLIN, D. R. Stump, J. HUSTON, H. L. Lai, P. NADOLSKY, W. K. Tung, J. High Energy Phys. **012** 0207 (2002).
- [35] J. F. Owens, Rev. Mod. Phys. **59** 465 (1987).
- [36] S. S. Adler et al., Phys. Rev. Lett. **98** 012002 (2007) .
- [37] J. Braun and H. Pirner, Phys. Rev. D **75** 054031 (2007).